Processed Kimberlite Porewater Geochemistry from Diavik Diamond Mines, Inc.

Michael C. Moncur[1,3] and Lianna J.D. Smith[2,3]

[1]Alberta Innovates-Technology Futures, Calgary, AB, CANADA, michael.moncur@albertainnovates.ca
[2] Rio Tinto - Diavik Diamond Mines Inc., Yellowknife, NT, CANADA, lianna.smith@riotinto.com
[3]University of Waterloo, Waterloo, ON, CANADA

Abstract
The mining of diamonds from kimberlite ore results in the production of processed kimberlite (PK) that is discharged as a slurry into a tailings impoundment. In 2009 and 2010, a study was initiated at the Diavik Diamond Mine to understand the evolution of porewater geochemistry in their PK tailings impoundment. Porewater was collected from a number of core and drive-point piezometers located across an exposed kimberlite beach and in the central pond and analysed for field parameters, dissolved cations and anions and nutrients. A subset of these samples was also analyzed for stable isotopes. Our results show that the lowest pH values and highest concentrations of dissolved SO_4 and metals were in the unsaturated zone of the PK impoundment. The pH values increased and dissolved SO_4 and metals concentrations decreased towards the water table. In the saturated zone average dissolved concentrations decreased by almost an order of magnitude compared to the unsaturated zone for SO_4, major cations and most metals (e.g SO_4: 3500 to 350 mg/L; Mg: 730 to 80 mg /L, Ni: 0.82 mg/L to 0.038 mg/L). PK porewater from the underlying frost zone showed a further increase in pH and decrease in dissolved SO_4 and metal concentrations.

Keywords: groundwater, permafrost, unsaturated zone, weathering, sulfide minerals, sulfur isotopes

Introduction
The development of diamond mines in Canada's North emphasizes the need to assess the environmental implications of storing processed kimberlite (PK) in regions with continuous permafrost. The Diavik Diamond Mine (Diavik) is located in the barren lands on an island in Lac de Gras, 300 km northeast of Yellowknife, NT, Canada (Figure 1). The mean annual temperature, rainfall, snowfall and lake evaporation at Diavik is -12^{0}C, 164 mm, 187 mm and 271 mm, respectively. Winter conditions persist from September through to June with a 1.5 to 5 m deep active layer developing during the warmer months.

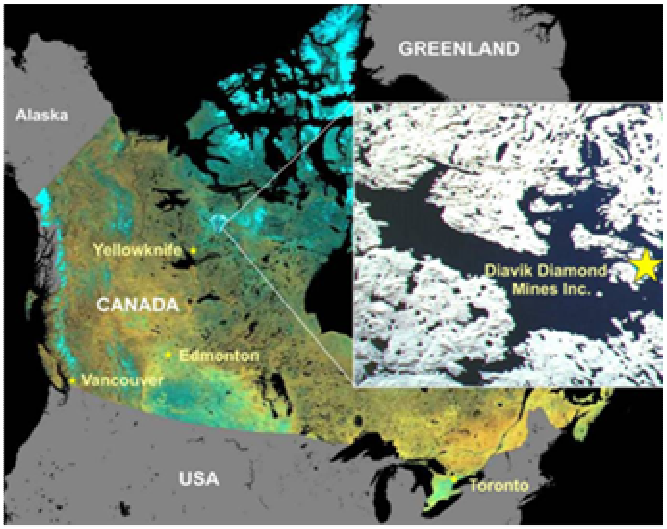

Figure 1. Location of Diavik Diamond Mine Inc., Northwest Territories, Canada.

Diavik started production in 2003 and approximately 6 million carats of gem-quality diamonds are extracted annually (Smith et al., 2011). During the life of the mine, up to 42 million tonnes of PK will be produced and require permanent storage. The objective of this study was to investigate groundwater chemistry in the Diavik Processed Kimberlite Containment (PKC) facility under conditions where the PK material was stored unsaturated, saturated, frozen and fully submerged.

Background

Diavik kimberlite ore occurs as three diamondiferous kimberlite pipes hosted in Archean granite and pegmatitic granite country rock of the Slave structural province (Moss et al., 2008). The pipes are composed of bedded volcaniclastic kimberlite, consisting of both kimberlite and mudstone xenoliths. Currently diamonds are extracted from the pipes through open pit and underground mining. After diamond are recovered from the kimberlite ore, the fine fraction (<1 mm) of the reject material is transported as a slurry to the PKC facitliy). Water from the processing plant is used in the PK slurry which contains both recycled PKC pond water and recycled open pit and underground seepage water. Processed kimberlite deposited in the PKC settles gravimetrically for permanent storage. The standing water in the PKC facility is decanted and recycled back to the processing plant. Treated sewage waste water from mining operations is also discharged to the PKC facility.

Mineralogy

The dominate minerals commonly found in the Diavik kimberlite include olivine [$(Mg,Fe)_2SiO_4$ with sub-percentage amounts of Ni], enstatite [$MgSiO_3$], chromium diopside [$Cr\text{-}CaMgSi_2O_6$], and lizardite [$Mg_3Si_2O_5(OH)_4$], with accessory minerals of garnet [$(Mg,Ca)_3(Al,Cr)_2(SiO_4)_3$], phlogopite [$KMg_3AlSi_3O_{10}(OH)_2$] and ilmenite [$FeTiO_3$] (Baker et al., 2003). Traces of pyrite [FeS_2], pyrrhotite [$Fe_{(1-x)}S$], sphalerite [(Zn,Fe)S], pentlandite [$(Fe,Ni)_9S_8$], chalcopyrite [$CuFeS_2$], galena [PbS], marcasite [FeS_2] and millerite [NiS] have been observed in the kimberlite material (Baker et al., 2003). Dominant and accessory minerals are set in a fine-grained, smectite-rich calcite and serpentine matrix. The mean-total sulfur value for the processed kimberlite is 0.52 % ± 0.24 % (Baker et al., 2003). Mean values of the neutralization potential (NP) and maximum potential acidity (MPA) for the processed kimberlite reported by Baker et al. (2003) were 196 ± 131 $CaCO_3$/t and 14.8 ± 6.6 $CaCO_3$/t, respectively, indicating that the processed kimberlite is acid-consuming.

Baker et al. (2003) found that the mudstone was fine-grained and composed of quartz [SiO_2], feldspar [$NaAlSi_3O_8$], muscovite [$KAl_2(AlSi_3O_{10})(F,OH)_2$], framboidal pyrite, calcite, smectite and gypsum [$CaSO_4 \cdot 2H_2O$]. The mean-total sulfur value for the mudstone is 0.70 % ± 0.86 %. Mean values of NP and MPA for the mudstone were 288 ± 186 $CaCO_3$/t and 19.93 ± 25.36 $CaCO_3$/t, respectively. Many of the mudstone samples had significantly lower NP and higher total S suggesting that the material is potentially acid generating.

Wilson et al., (2009) observed efflorescent crusts of secondary minerals on the surface of PKC facility where the PK was beached adjacent to the ponded water. Calcite, gypsum [$CaSO_4 \cdot 2H_2O$] and nesquehonite [$Mg(HCO_3)(OH) \cdot 2H_2O$] were the most pervasive secondary mineral phases in the PKC facility post deposition. Other secondary Ca-Mg mineral phases identified in trace amounts within the PK material include anhydrite [$CaSO_4$], epsomite [$MgSO_4 \cdot 7H_2O$], hexahydrite [$MgSO_4 \cdot 6H_2O$], syngenite [$K_2Ca(SO_4)_2 \cdot (H_2O)$], gaylussite [$Na_2Ca(CO_3)_2 \cdot 5H_2O$], natrite [$Na_2CO_3$], vaterite ($CaCO_3$) and portlandite [$Ca(OH)_2$]. Nesquehonite was the only secondary mineral identified to persist at depth within the PKC facility.

Methods

In 2009 five piezometer nests were installed across the East Beach of the PKC facility, extending 200 m from the toe of the containment dam to the edge of ponded water (Figure 2). Each nest contained 1 to 3

piezometers driven to refusal with a gas-powered rock hammer. At all piezometer-nest locations, three sets of continuous core of the tailings were collected from surface to the frost layer or refusal, using the method of Starr and Ingleton (1992). One set of core was cut into 20 to 25 cm lengths, and then sampled to determine pore-water composition using a squeezing technique described by Patterson et al. (1978), later modified by Blowes et al. (1991). Additional collected core was analyzed for moisture content and sieve analysis. Detailed methods of piezometer installation, groundwater sampling, pore-water squeezing and groundwater sampling used at the PKC facitliy were identical to those described by Moncur et al. (2005).

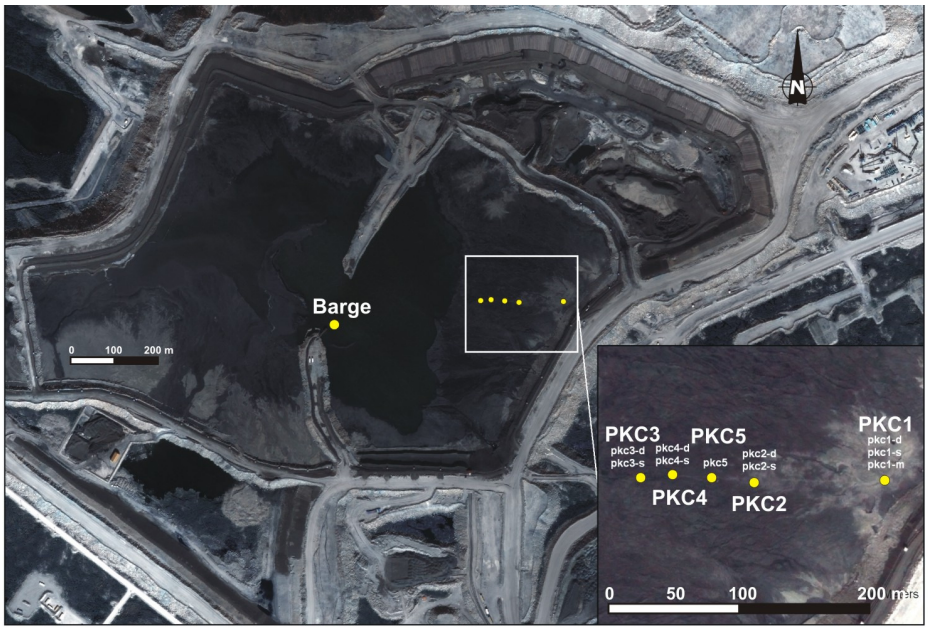

Figure 1. Aerial view of the PKC facility (2009) showing piezometer nest locations.

An additional location was investigated at end of the Barge where groundwater could be collected from beneath standing water of the PKC water column (Barge). In 2009 five piezometers were installed from Barge ranging in depth from 7 m to 25 m below the pond surface. The Barge location had to be re-instrumented in 2010 due to rising water levels in the PKC pond.

Field parameters measured from all piezometers and the PKC surface water included pH and Eh measured in a sealed flow-through cell, alkalinity, temperature and electrical conductivity. Dissolved concentrations of H_2S, NH_3, Fe(II), and PO_4 were measured in the field using a Hach DR2700 spectrometer. All water samples were passed through 0.45 µm cellulose-nitrate filters and stored in pre-washed Nalgene bottles. Water samples were immediately refrigerated until analyses for major anions, cations and metals at the University of Waterloo. $\delta^{34}S$ and $\delta^{18}O$ values of dissolved SO_4 were measured from 9 groundwater samples and 1 surface water sample from the PKC facility. In addition, 1 kimberlite and 3 mudstone samples were analyzed for $\delta^{34}S$ at the University of Calgary.

Groundwater and surface water chemistry was interpreted with the assistance of the equilibrium chemical-speciation/mass-transfer model MINTEQA2 (Allison et al., 1990). The MINTEQA2 data base was modified to make it consistent with that of WATEQ4F (Ball and Nordstrom, 2001). MINTEQA2 was used to calculate the saturation indices for discrete minerals that may be controlling the concentrations of dissolved species in waters of the PKC facility.

Samples of PK pore gas from the unsaturated zone were collected at locations PKC1 in September 2009 and then again resampled in August 2010, using a drive-point sampling tube. Pore gas was collected in 60 CC syringes at 10 cm increments from ground surface to the depth of 100 cm. Gas-loaded syringes collected from each sampling interval were immediately injected into sterile vacuum-sealed Kendall 16x125 mm glass vials. Gas content from the vials was analyzed for O_2, CO_2, CH_4, N_2 and H_2S using a Varian CP-4900 Micro Gas Chromatograph.

Results and Discussion

PKC Facility – East Beach

Exposed PK material on the East Beach gently sloped from the toe of the rock dam to the Pond edge with a 4.15 m change in elevation. Figure 3 shows cross-sections through the east beach from PKC1 to PKC3. In July 2009, depth to frost was 1.13 m at PKC1 and 0.96 m at PKC3. By September 2009, the active zone at had increased to 1.70 m at PKC1 and 1.23 m at PKC3, however there was minimal change in the depth to frost over the same time period at locations PKC2 and PKC5.

Depth to the water table in the PKC facility was 1.25 m below the PK surface at PKC1, and intersected the surface near PKC4. Groundwater had a downward gradient at locations PKC1 and PKC2 and showed an upward gradient at location PKC4, indicating that groundwater flow was directed downwards from the toe of the east dam to the PKC Pond. The overall horizontal gradient between PKC1 and PKC3 was 0.016, following the topography of the ground surface. Grain-size distributions were measured on 10 samples extracted from various depths across the PKC beach. The average d_{10} (the grain-size diameter at which 10% by weight of the particles are finer in mm) of the PK material varied between 0.01 mm to 0.12 mm. Hydraulic conductivities (K) of the PKC material were estimated using the method developed by Beyer, which is suitable for sediments with a d_{10} within the range of 0.06 mm < d_{10} <0.6 mm (Vukovic and Soro, 1992). The arithmetic average hydraulic conductivity calculated from the grain-size analysis was 2.54×10^{-5} m/s and the average calculated porosity was 0.30. These values were used with the water table gradient between PKC1 and PKC3 in the Darcy equation to estimate groundwater velocities of about 1.3×10^{-5} m/s (42 m/a).

Measured values of pore water Eh and concentrations of selected dissolved major ions and metals versus depth across the unsaturated zone (Figure 3) showed that the unsaturated zone was the most oxidized zone in the cross-section. This zone also had the lowest pH values (>7.01) and much higher concentrations of dissolved sulfate (<6800 mg/L) and metals than other waters sampled in the PKC facility (Moncur Groundwater, 2009). There were decreases in dissolved sulfate and metal concentrations and increases in pH as the water table was approached and within the frost zone.

Distinct differences in the average concentration of pH, Eh and dissolved ions from the unsaturated zone, saturated zone and the frost zone are shown in Table 1. Differences in Eh measurements indicate oxidizing conditions in the unsaturated zone that become progressively more reduced with depth into the frost zone. The shift towards more reduced conditions with depth corresponds with a shift towards increasing pH values. Average dissolved concentration of sulfate, most major cations and metals decreased by almost an order of magnitude from the unsaturated zone to the saturated zone (e.g. SO_4: 3500 to 350 mg/L, Mg: 730 to 80 mg/L, Ni:820 to 38 µg/L). The concentrations of dissolved ions were significantly lower in the frost zone than in the saturated zone. Alkalinity concentration ranges (in mg/L of $CaCO_3$) were similar in the unsaturated and saturated zones, but increased in the frost zone. Ions that show little variation between the three zones include Cl and K.

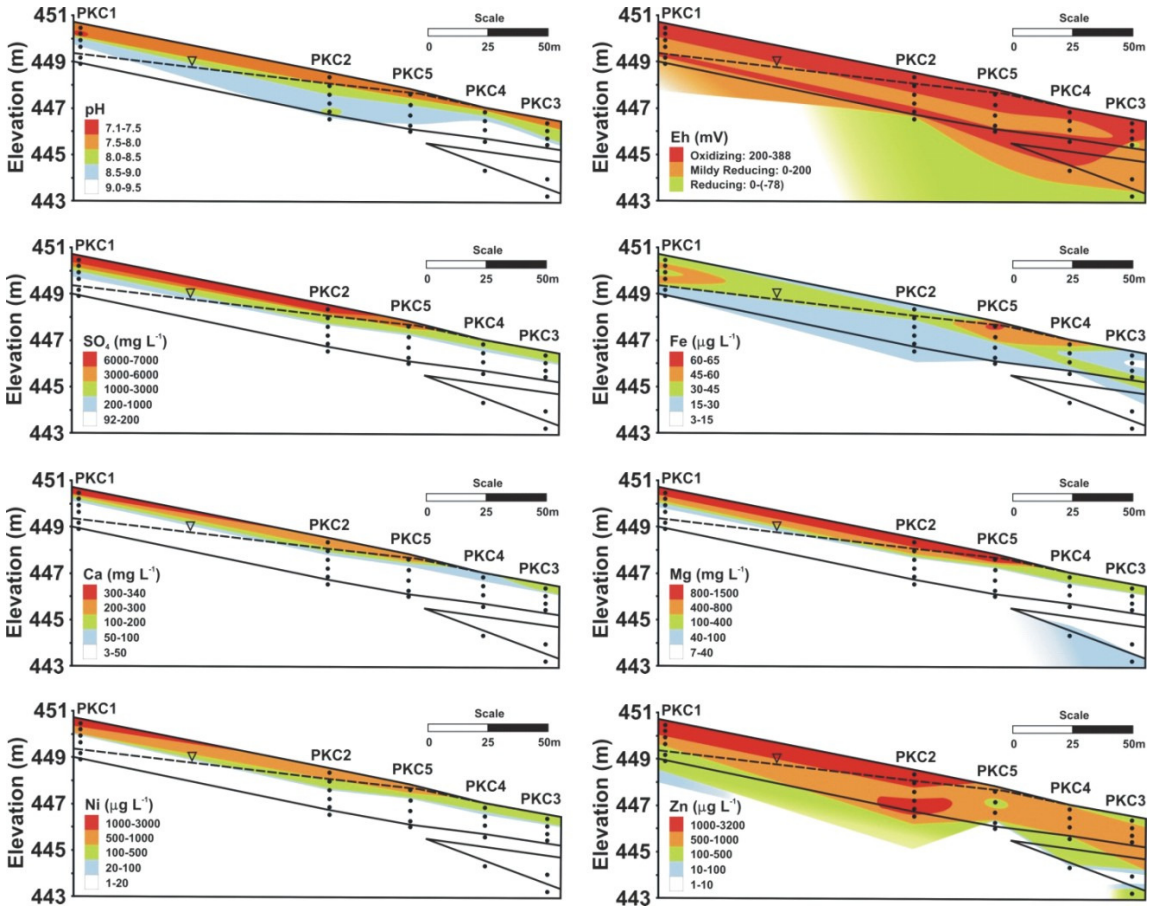

Figure 3. Water chemistry across the East Beach of the PKC facility. Black dots represent discrete porewater sampling locations and the dashed line with inverted triangle corresponds to the water table elevation. The lower solid line represents the depth to frost and the wedge to the right is a frost-free zone.

Table 1. Maximum, minimum and average concentrations of dissolved ions measured from the unsaturated zone (UZ), saturated zone (SZ) and frost zone (FZ).

Location	*pH*	*Eh (mV)*	*Alkalinity (mg/L)*	*SO_4 (mg/L)*	*Ca (mg/L)*	*Mg (mg/L)*	*Fe (µg/L)*	*Ni (µg/L)*
Average UZ	**8.05**	**272**	**66**	**3500**	**164**	**730**	**41**	**819**
Max UZ	*9.06*	*388*	*85*	*6800*	*338*	*1490*	*65*	*2950*
Min UZ	7.01	191	52	100	5	7	26	2
Average SZ	**8.80**	**188**	**66**	**350**	**21**	**80**	**24**	**38**
Max SZ	*9.41*	*344*	*100*	*2400*	*129*	*505*	*58*	*312*
Min SZ	7.84	-46	47	90	4	15	3	1
Average FZ	**9.17**	**136**	**83**	**170**	**8**	**28**	**10**	**11**
Max FZ	*9.48*	*231*	*110*	*300*	*17*	*65*	*39*	*30*
Min FZ	8.95	-78	40	90	2	8	3	1

Elevated concentrations of dissolved ions within the unsaturated zone are likely the result of weathering reactions. Elevated concentrations of dissolved SO_4 and some metals may be due to microbially mediated oxidation of sulfide minerals within the PK material. Figure 4 shows a profile of pore gas concentrations measured from the PK surface to a one meter depth at location PKC1. Oxygen concentrations were at atmospheric (20.9%) from the surface to a depth of 0.5 m at which point the oxygen concentrations decreased to 3% at a 1 m depth. As discussed earlier, a number of sulfide minerals have been identified in

the kimberlite and mudstone materials. Consumption of oxygen by the oxidation of sulfide minerals is represented through:

Pyrite: $$FeS_2 + \tfrac{15}{4} O_2 + \tfrac{7}{2} H_2O \rightarrow 2SO_4^{2-} + Fe(OH)_3 + 4H^+ \quad (1)$$

The oxidation of pyrite results in the release of 2 moles of sulfate, 4 moles of acid and a ferric (oxy)hydroxide precipitate. Speciation modeling results show that the porewater at location PKC1 was supersaturated with respect to secondary ferric (oxy)hydroxide minerals, suggesting theses phases may control dissolved Fe concentrations (Figure 5). Column experiments using the PK material have identified goethite as a secondary precipitate (Baker et al., 2003).

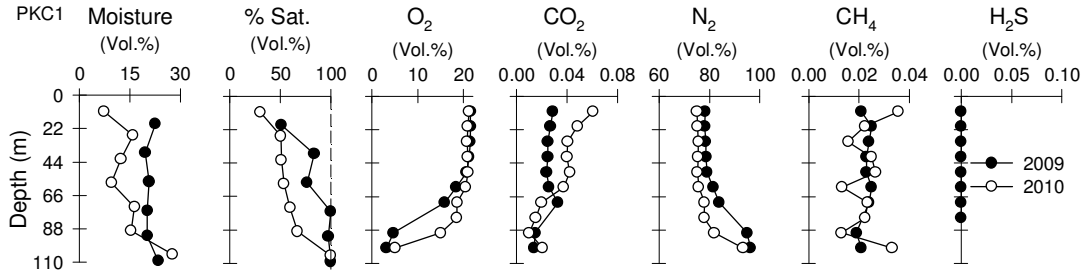

Figure 4. Depth profiles of soil moisture and pore gas measured from the unsaturated zone at location PKC1.

Another cause for the decrease in O_2 gas concentration with depth was the increase in water content with depth in the PK material. In 2009 the O_2 content at PKC1 showed an abrupt decrease at 70 cm which coincides with almost complete saturation of the PK material at that depth (Figure 4). Gas measurements in 2010 from PKC1 showed a decrease in O_2 gas concentration at 90 cm, again corresponding with saturation of the PK material. These results demonstrate that water content of the PK material controlled the depth of O_2 diffusion.

Dissolved concentrations of metals in the unsaturated zone were lower than expected due to the high neutralizing potential of the PK material. The pH of the porewater and groundwater remained neutral, limiting the solubility of most metals. Calcite makes up between 4 to 8 wt % of the PK providing neutralization values of 39 to 85 kg $CaCO_3$ eq/t, far exceeding acid generating potentials of pyrite estimated to be in the 5 to 12 kg $CaCO_3$ eq/t (Paktunc and Thibault, 2010). The dissolution of calcite maintains the pH of the porewater near neutral through dissolution:

Calcite: $$CaCO_3 + H^+ \leftrightarrow Ca^{2+} + HCO_3^- \quad (2)$$

where one mol of acid is consumed and one mol of Ca and HCO_3 are released to the porewater. This reaction may account for some of the elevated concentrations of dissolved Ca in the unsaturated zone. Geochemical modeling results showed that the porewater approaches or is at saturation with respect to calcite (Figure 5). Under neutral conditions, other minerals in the PKC facility, such as phlogopite, may undergo incongruent dissolution releasing dissolved Mg to the porewaters (Murakami et al., 2003):

Phlogopite: $$K(Mg_2Fe)(AlSi_3)O_{10}(OH)_2 + 5H^+ + 0.25O_2 + 3H_2O \rightarrow 0.5Al_2Si_2O_5(OH)_4 + Fe(OH)_3 + 2H_4SiO_4 + K^+ + 2Mg^{2+} \quad (3)$$

Within the unsaturated zone, Ca and Mg concentrations were highest near the PK surface. Phlogopite was identified in the PK material (Baker et al., 2003; Paktunc and Thibault, 2010) and the porewater in the unsaturated zone was at satuation with respect to phlogopite (Figure 5).

In acid-neutralizing carbonate-mineral dissolution reactions the depletion of O_2 concentrations in pore gas is typically accompanied by an increase in CO_2 concentrations (Blowes et al., 1998). However, at PKC1 as O_2 concentrations decreased with depth the CO_2 concentrations also decreased to levels below atmospheric (0.036%) (Figure 4), suggesting that the CO_2 was being sequestered. This is consistent with previous work showing that dissolution of silicate minerals within the PKC facility is sequestering CO_2 through the precipitation of carbonate mineral phases (Wilson et al., 2009). The possible dissolution of common silicate minerals like olivine and lizardite in the PKC facility can be represented by the equations:

Olivine: $$(Mg,Fe)_2SiO_4 + 5/2O_2 + CO_2 + 5H_2O \rightarrow 2MgCO_3 + 2Fe(OH)_3 + Si(OH)_4 \quad (4)$$

Lizardite: $$Mg_3Si_2O_5(OH)_4 + 3CO_2 \rightarrow MgCO_3 + 2SiO_2 + 2H_2O \quad (5)$$

Speciation modeling suggests that porewater was undersaturated with respect to olivine. The dissolution of the minerals in equations (4) and (5) would result in the precipitation of magnesite [$MgCO_3$], which is consistent with equilibrium calculations that show the porewaters at location PKC1 were at saturation with respect to magnesite (Figure 5). The dissolution of Ni-bearing olivine will also release dissolved Ni to the porewaters including dissolved concentrations of Mg.

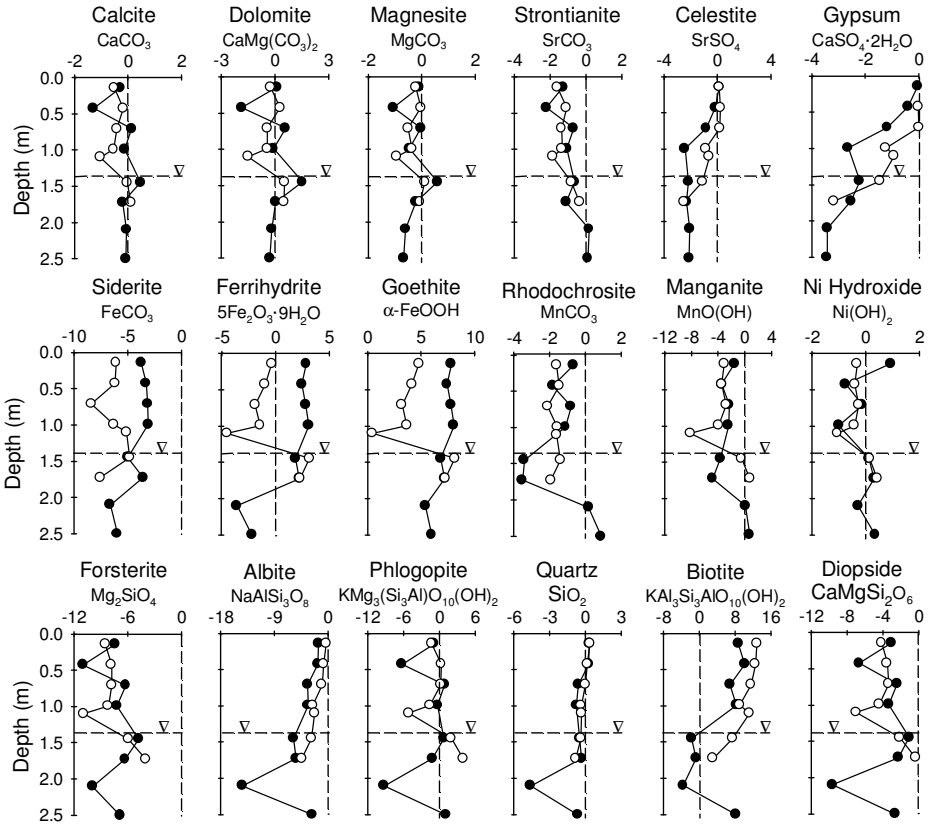

Figure 5. Depth profiles of saturation indices from PKC1.Horizontal dashed line with the inverted triangle represents the water table. Solid circles were measured in 2009 and open circles 2010.

PKC Barge

Water levels in four nested Barge piezometers were measured relative to the water level in the adjacent PKC pond in September 2011 (Table 2). The water levels in all piezometers were flowing over the casing tops indicating a strong upward gradient or positive head.

Table 2. Water levels measured from the nested Barge piezometers in September 2011 with respect to the water surface of the PKC pond. Water from all piezometers was flowing over top of casing.

Location	*Depth (m)*	*Water Level (m above pond level)*
Barge-20	6.1	1.00
Barge-30	9.1	1.06
Barge-40	12.2	1.04
Barge-55	16.8	1.46
Barge-75	22.9	1.49

The hydraulic conductivity (K), measured from the five Barge piezometers using rising-head piezometer-response tests and calculated using the method of Hvorslev (1951), ranges from 7.8×10^{-8} m/s to 7.2×10^{-10} m/s, with an average of 3.5×10^{-8} m/s. The K value of the PK material at the Barge is far lower than than measured from the PKC East Beach material. The difference in K is due to differential settling during deposition of the PK material. The beach material is closer to the spigot discharge point resulting in the deposition of a sand-size fraction of PK material whereas the Barge is more distal from the discharge point resulting in an accumulation of a clay-size fraction of PK material.

Profiles of groundwater chemistry collected in 2009 and 2010 from the Barge piezometers show concentrations of dissolved ions, and Eh were generally higher in the PKC pond water, and decrease with depth though the PK material (Figure 6). The distributions of major anions and cations and trace metals displayed little change between 2009 and 2010. In 2009 dissolved Zn concentrations showed a significant increase with depth, however dissolved Zn concentrations were below detection during sampling in 2010, suggesting possible analytical uncertainty. Speciation modeling results show that carbonate minerals are at saturation near the surface and bottom of the profile and (oxy)hydroxide mineral phases are at saturation across the central portion of the profile (Figure 7). These secondary mineral phases may be controlling pH and the dissolved concentration of ions in the porewater.

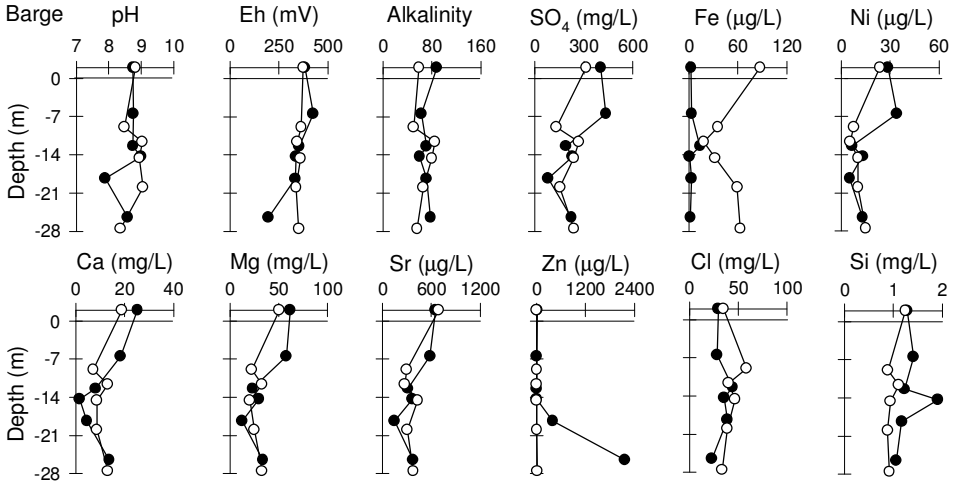

Figure 6. Depth profile of groundwater chemistry from the Barge location measured in 2009 and 2010.The top point represents PKC pond chemistry and the horizontal solid line is the boundary between the surface water column and PKC material. Solid circles were measured in 2009 and open circles 2010.

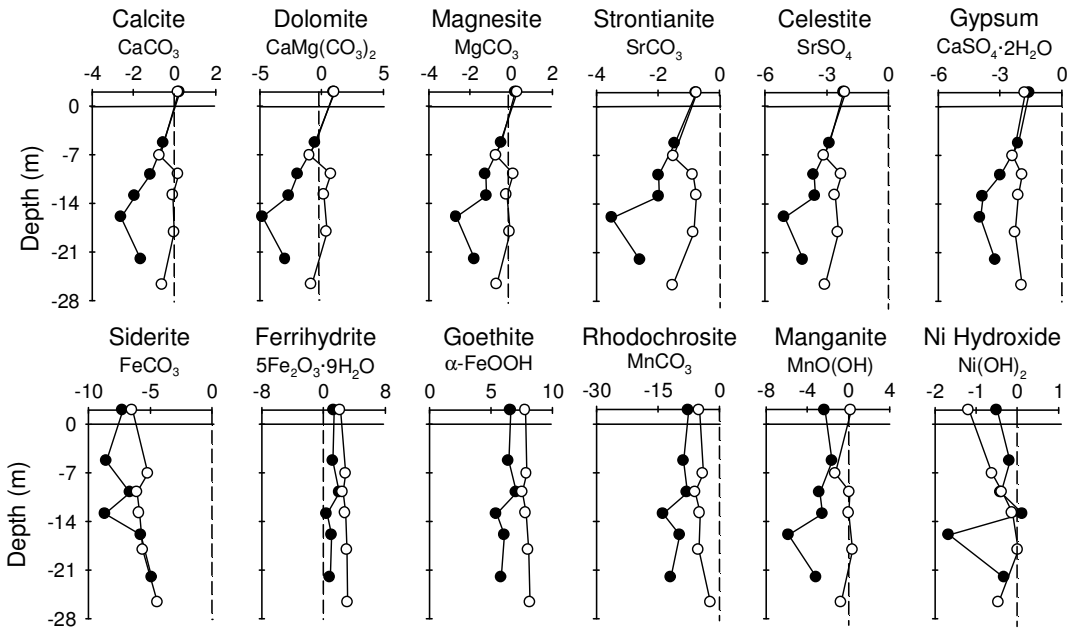

Figure 7. Depth profile of saturation indices from the Barge piezometers calculated using MINTEQA2. The upper point represents the PKC pond chemistry and the solid horizontal line is the boundary between the surface water column and PKC material. Closed circles represent 2009 and open circles are from 2010.

Concentrations of dissolved ions measured from the Barge piezometers were much lower than concentration measured from the porewater in the unsaturated zone of the East Beach. Even though the subaqueous tailings at the Barge received similar materials as the East Beach exposed PK, the difference between geochemical profiles indicates that the subaqueous disposal PK material has significantly limited weathering and the subsequent release of ions to the porewaters. The ability of a water cover to reduce the ingress of O_2 into tailings and the subsequent mineral weathering is well recognized and subaqueous disposal of mine tailings is a common practice in tailings management (eg. Pedersen et al., 1993; Vigneault et al., 2001; Jacob and Otte, 2004; Samad and Yanful, 2005). The O_2 ingress into the tailings is limited by the slow diffusion of O_2 through the water cover. For example, the diffusive flux of O_2 to water covered tailings is almost 10 000 times less than uncovered tailings (Robertson et al., 1997).

$\delta^{34}S_{SO4}$ isotopic ratios

The δ^{34}S-SO_4 values of the various rock types in the PK material and the δ^{34}S-SO_4 and δ^{18}O-SO_4 composition of the PKC waters collected at the East Beach, Barge and PKC pond can be used to improve our understanding of the sources of SO_4 to in the PKC tailings and pond (Figure 8). The potential sources of SO_4 to the porewaters and pond include dissolution of sulfate minerals inherent in the kimberlite or oxidation of sulfides. Gypsum has been identified in the Diavik kimberlite (Baker et al., 2003) and PK (Wilson et al., 2009) and previous work has suggested that elevated SO_4 concentrations in the PK porewater at the nearby Ekati Mine was due to dissolution of a calcium sulfate mineral (Rollo and Jamieson, 2006). A number of sulfide minerals have been identified in the PK material including pyrite and pyrrhotite (Paktunc and Thibault, 2010). Samples of gypsum from the PK material were not available for δ^{34}S analysis, but the δ^{34}S-SO_4 value of tertiary aged $CaSO_4$ is typically enriched, around +20‰ (Clark and Fritz, 1997). The δ^{34}S-SO_4 of the solid unprocessed kimberlite was -21.0 ‰ and the mudstone ranged from -20.4 to -46.4 ‰. Negative δ^{34}S values are typical of diagenetic environments where reduced sulfur compounds are formed, with the most common reaction product being pyrite (Clark and Fritz, 1997). The δ^{34}S-SO_4 values of the PK porewater overlap the ranges for unprocessed kimberlite and mudstone with values -15.3 to -21.8‰. The similarity between the PK porewater and the unprocessed kimberlite and mudstone indicate minimal fractionation between the solid phase and dissolved phase which is consistent

with previous studies (Taylor et al., 1984; Edraki et al., 2005). Gypsum identified in the Diavik PKC facility was identified as a secondary product from weathering of the PK material (Wilson et al., 2009). The $\delta^{34}S\text{-}SO_4$ values measured in the porewater of the Diavik PK material are strongly depleted (-19‰) suggesting that the primary source of dissolved SO_4 is sulfide oxidation. The dissolution of sulfate mineral phases cannot be excluded as a minor source of sulfate to the porewater, however only trace amounts of a sulfate mineral ($BaSO_4$) were observed during mineralogical examination of the PK material compared to more abundant pyrite (Paktunc and Thibault, 2010).

There was also very little variation in the PKC porewater $\delta^{34}S\text{-}SO_4$ signatures with depth, between the different redox zones and or between water with large differences SO_4 concentrations. The absence of a positive shift in $\delta^{34}S$ values typically associated with microbially mediated sulfate reduction could be the result of the high SO_4:H_2S ratio. The sample from the PKC pond and the PKC porewater samples all have $\delta^{34}S\text{-}SO_4$ and $\delta^{18}O\text{-}_{SO4}$ signatures consistent with the sulfate originating from the oxidation of sulfide minerals.

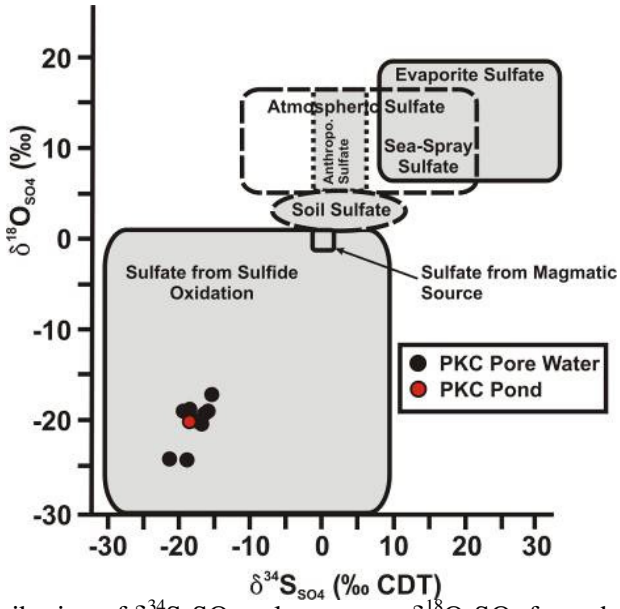

Figure 8**.** Plot showing distribution of $\delta^{34}S\text{-}SO_4$ values versus $\delta^{18}O\text{-}SO_4$ from the PK pore water (revised after Mayer, 2005). CDT: Cañon Diablo Triolite

Conclusions

The following conclusions were made:

- Frost Zone
  - The active, frost-free zone is below a depth of 1 m across the East Beach. Between July 2009 and September 2009, the active zone increased in depth by 0.57 m and 0.27 m at locations PKC1 and PKC3, respectively.
  - During piezometer installation below the PKC pond water column at the Barge in 2009 and 2010, no frost was encountered from surface to a depth of 25 m.
  - The concentrations of dissolved ions were significantly lower in the frost zone than in the saturated and vadose zones.

- Processed Kimberlite Groundwater Geochemistry
  - Moisture content in the PK material limited the depth of O_2 diffusion and is an important control on the depth of weathering.

- The highest concentration of dissolved metals, major cations and sulfate were measured in the unsaturated zone of the PKC facility. Dissolved ion concentrations are likely due to weathering processes. However, the concentrations of metals in the unsaturated zone at the PKC facility are relatively low due to the high neutralizing potential of the PK material, which keeps the pH of the porewater and groundwater near neutral and limits the solubility of most metals. Dissolution of carbonate minerals and phlogopite is consistent with the elevated concentrations of dissolved Ca in the unsaturated zone.
- Even though the sub-aqueous tailings at the Barge site received fairly similar materials as the aerially exposed East Beach tailings, the difference between geochemical profiles indicates that the subaqueous disposal PK material has significantly limited weathering and the subsequent release of ions to the porewaters.
- Groundwater collected from Barge and water extracted from the frost zone had the lowest concentration of dissolved ions.
- The $\delta^{34}S\text{-}SO_4$ values measured in porewater from the PK material were strongly depleted (-19‰) and showed minimal fractionation from unprocessed kimberlite (-21‰) suggesting that the source of SO_4 is most likely a product of sulfide oxidation.
- Speciation modeling shows that the main minerals controlling the pH and dissolved ions are secondary carbonate and (oxy)hydroxide minerals. Secondary sulfate minerals may control SO_4 and other metals at the near surface in unsaturated areas of the PKC facility.
- The subaqueous disposal and freezing of the PK material limits the ingress of atmospheric O_2 subsequently limiting the release of dissolved concentrations of metals and SO_4 to the adjacent porewater.

Acknowledgements

Special thanks to Rio Tinto-DDMI for funding and allowing us to present this study. The authors graciously thank Stacey Hannam, Jean Birks, David Blowes, Kent Richardson, Scott Jasechko, Jeff Bain, John Gibson, Dogan Paktunc and Norm Costanza for their technical assistance and advice. The authors thank Graeme Campbell and two anonymous reviewers for their constructive criticism.

References

Allison, J.D., Brown, D.S. and Nova-Gradac, K.L. (1990) MINTEQA2/PRODEFA2, a Geochemical Assessment Model for Environmental Systems, Version 3.0 User's Manual, Report EPA/600/3-91/021, Environmental Research Laboratory, Office of Research and Development, U.S. Environmental Protection Agancey, Athens, GA, p. 106.

Baker, M.J., Blowes, D.W., Logsdon, M.J. and Jambor, J.L. (2003) Environmental geochemistry of kimberlite materials: Diavik Diamond Project, Lac de Gras, Northwest Territories, Canada. Exploration Mining Geology, Vol. 10, pp. 155-163.

Ball, J.W. and Nordstrom, D.K. (2001) User's manual for WATEQ4F with revised thermodynamic data base and test cases for calculating speciation of major, trace and redox elements in natural waters, Report 91-183, U.S. Geolological Survey Open-File, p. 188.

Blowes, D.W., Reardon, E.J., Jambor, J.L. and Cherry, J.A. (1991) The formation and potential importance of cemented layers in inactive sulfide mine tailings. Geochimica Cosmochimica Acta, Vol. 55, pp. 965-978.

Blowes, D.W., Jambor, J.L., Hanton-Fong, C.J., Lortie, L. and Gould, W.D. (1998) Geochemical, mineralogical and microbiological characterization of a sulphide-bearing carbonate-rich gold-mine tailings impoundment, Joutel, Québec. Applied Geochemistry, Vol. 13, pp. 687-705.

Clark, I.D. and Fritz, P. (1997) Environmental Isotopes in Hydrogeology. Lewis, Baton-Rouge, p. 328.

Edraki, M., Golding, S.D., Baublys, K.A. and Lawrence, M.G. (2005) Hydrochemistry, mineralogy and sulfur isotope geochemistry of acid mine drainage at the Mt. Morgan mine environment, Queensland, Australia. Applied Geochemistry, Vol. 20, pp. 789-805.

Hvorslev, M.J. (1951) Time lag and soil permeability in ground-water observations., Bulletin No. 36, U.S. Army Corps of Engineers, Waterways Experiment Station, Vicksburg, MS, pp. 1-50.

Jacob, D.J. and Otte, M.L. (2004) Long-term effects of submergence and wetland vegetation on metals in a 90-year old abandoned Pb-Zn mine tailings pond. Environmental Pollution, Vol. 130, pp. 337-345.

Moncur, M.C., Ptacek, C.J., Blowes, D.W. and Jambor, J.L. (2005) Release, transport and attenuation of metals from an old tailings impoundment. Applied Geochemistry, Vol. 20, pp. 639-659.
Moncur Groundwater, 2009. PKC mass balance study, Diavik Diamond Mines Inc., Diavik, Northwest Territories. Internal report prepared for DDMI.
Mayer, B. (2005) Assessing sources and transfromations of sulfate and nitrate in the hydrosphere using isotope techniques. Isotopes in the Water Cycle: Past, Present and Future of a Developing Science. P.K. Aggarwal, J.R. Gat, K.F.O. Froehlich (Eds.), International Atomic Energy Agency, Springer, Dordrecht, Netherlands, p. 67-89.
Murakami, T., Utsunomiya, S., Yokoyama, T. and Kasama, T. (2003) Biotite dissolution processes and mechanisms in the laboratory and in nature: Early stage weathering environments and vermiculitization. American Mineralogist, Vol. 88, pp. 377-386.
Moss, S., Russell, J.K. and Andrews, G.D.M. (2008) Progressive infilling of a kimberlite pipe at Diavik, Northwest Territories, Canada: Insights from volcanic facies architecture, textures, and granulometry. Journal of Volcanology and Geothermal Research, Vol. 174, pp. 103-116.
Paktunc, A.D. and Thibault, Y. (2010).. Quantitive mineralogy of processed kimberlite and waste rock samples from the Diavik Diamond Mines. Internal report prepared for DDMI.
Patterson, R.J., Frape, S.K., Dykes, L.S. and McLeod, R.A. (1978) A coring and squeezing technique for the detailed study of subsurface water chemistry. Canadian Journal of Earth Sciences, Vol. 15, 1pp. 62-169.
Pedersen, T.F., Mueller, B. and McNee, J.J. (1993) The early diagenesis of submerged sulphide-rich mine tailings in Anderson Lake, Manitoba. Canadian Journal of Earth Sciences, Vol. 30, pp. 1099-1109.
Robertson, J.D., Tremblay, G.A. and Fraser, W.W. (1997) Subaqueous tailings disposal: A sound solution for reactive tailings. In: 4th International Conference on Acid Rock Drainage, May 31-June 6, Vancouver, BC, Canada, Vol. 3, p. 1027-1044.
Rollo, H.A. and Jamieson, H.E. (2006) Interaction of diamond mine waste and surface water in the Canadian Arctic. Applied Geochemistry, Vol. 21, pp. 1522-1538.
Samad, M.A. and Yanful, E.K. (2005) A design approach for selecting the optimum water cover depth for subaqueous disposal of sulfide mine tailings. Canadian Geotechnical Journal, Vol. 42, pp. 207-228.
Smith, L.J.D., Moncur, M.C., Neuner, M., Gupton, M., Blowes, D.W., Smith, L. and Sego, D.C. (2011) Design and construction of field-scale instrumented waste rock piles in the Canadian arctic. In press Applied Geochemistry.
Starr, R.C. and Ingleton, R.A. (1992) A new method for collecting core samples without a drill rig. Ground Water Monitoring and Remediation, Vol. 41, pp. 91-95.
Taylor, B.E., Wheeler, M.C., and Nordstrom, D.K. (1984) Isotope composition of sulfate in acid mine drainage as measure of bacterial oxidation. Nature, Vol. 308, pp. 538-541.
Vigneault, B., Campbell, P.G., Tessier, A. and De Vitre, R. (2001) Geochemical changes in sulfidic mine tailings stored under a shallow water cover. Water Research, Vol. 35, pp. 1066-1076.
Vukovic, M., Soro, A., 1992. Determination of Hydraulic Conductivity of Porous Media from Grain-Size Composition. Water Resources Publications, Littleton, Colorado, USA.
Wilson, S.A., Raudsepp, M. and Dipple, G.M. (2009) Quantifying carbon fixation in trace minerals from processed kimberlite: A comparative study of quantitative methods using X-ray powder diffraction data with applications to the Diavik Diamond Mine, Northwest Territories, Canada. Applied Geochemistry, Vol. 24, pp. 2312-2331.

Acronyms

PK: Processed Kimberlite
PKC: Processed Kimberlite Containment
NP: Neutralization Potential
MPA: Maximum Potential Acidity
CDT: Cañon Diablo Triolite
US: Saturated Zone
SZ Unsaturated Zone
FZ: Frost Zone